

The Milky Way

AA2051

Available as a module for a *University Advanced Certificate*,
CertHE, *DipHE* and *BSc in Astronomy*.

Sample Notes

These sample pages from the Course Notes for the module *The Milky Way* have been selected to give an indication of the level and approach of the course. They are not designed to be read as a whole, but are intended to give you a flavour of the syllabus, style, diagrams, images, equations, mathematical content and presentation. They are a subset of the colour, navigable on-line version of the learning materials.

The Course Notes and other learning materials are made available via the course website.

- All sections of notes will be available in modest colour and basic navigation in pdf format suitable for downloading and printing at home.

July 2008

Instead it transpired that a far more efficient obscuration process was at work in interstellar space, due to the presence of smoke-like particles subsequently called **interstellar dust**. Interstellar dust was not discovered until 1930, via a series of observations of open clusters made by Trumpler. We will discuss interstellar dust and gas in greater depth in *Section 5 of this module*. Suffice it to say here that the presence of interstellar dust explained why Kapteyn's model was wrong and why Shapley's model was much more accurate. Shapley's model depended strongly on Globular Cluster observations and these were far less affected by dust because the dust is strongly concentrated in the Galactic disc.

Current models for the Milky Way

Current models and observations suggest the Milky Way Galaxy is an **Sbc-Sc type** spiral galaxy. Examples of face-on views of Sc and Sbc spirals are shown in Figure 1.3 and *Sc&G* Figures 5.10 and 5.25, whilst their Figure 5.16 shows an edge-on view of an Sc galaxy. For comparison, the nearest external spirals, M31 and M33, are respectively classified as Sb and Sc-Scd. Hence the Galaxy is considered to be intermediate in type between these two local spirals: see *Sc&G* Figure 4.1, which shows a montage of images of local galaxies drawn to the same linear scale and to the same level of surface brightness.

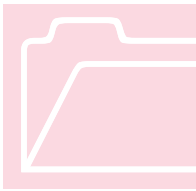


Figure 1.3
Hubble Space
Telescope image of the
nearby Sb spiral galaxy
NGC 3310.
Credit: [NASA](#)² and The
Hubble Heritage Team
([STScI](#)/[AURA](#))



There is also some evidence that our Galaxy has a relatively small central linear bar structure, extending to about 3 kpc from the centre. This is analogous to those bars seen in at least one-third of all spiral galaxies, though not dominant enough to place us on the Hubble barred-spirals (SB) sequence. Spiral structure, the probable bar, and the contents of the nucleus of the Galaxy will be studied in *Sections 6 and 8 of this module*.

² Public domain HST image from <http://opposite.stsci.edu/pubinfo/>

It is useful to divide the structural description of the Galaxy into the following convenient components. These are mainly morphological structures and may be considered as separate components for study, though in practice there is overlap between some of them. In general, we follow the nomenclature of *SEG* (see their section 1.2 for a further brief introduction to some of these features, which are located on a schematic edge-on sketch view of the Galaxy in their Figure 1.8).

- **Thin disc** (young population I stars)
- **Warp** and flare of the disc
- **Local concentrations** and co-moving groups *e.g.* Gould's Belt
- **Spiral arms**; spiral density wave pattern
- **Interstellar gas and dust** including supernova remnants
- **Thick disc** (intermediate population stars)
- **Inner halo** including relatively metal-rich globular clusters
- **Metal-poor halo**, including metal-poor globular clusters (old population II stars)
- **Hot gas and high-velocity clouds**, high-latitude dust (cirrus)
- **Bulge**
- **Bar**
- **Nucleus**
- Central massive **black hole**
- **Dark matter halo**
- **External influences** on the Galaxy, including intergalactic streams, and mergers/interactions of Local Group galaxies with the MW Galaxy.

Each of these components and structures (except the last item) will be studied in some detail in relevant later sections in this *Milky Way Galaxy module*, beginning with the region of the solar neighbourhood in *Section 2*.

Population types and metallicity

A classification of stars into two basic Population Types (**Population I and II**) was originally suggested by Baade in 1944, based on observations of individual stars in nearby external spiral and elliptical galaxies. The classification was later extended to stars in the Galaxy. The observational classification distinguished luminous blue stars in galactic discs and spiral arms (Pop I) from luminous red stars which predominate in elliptical galaxies and also in the bulges and globular clusters in spiral galaxies. The fundamental physical distinction is one of age and **chemical composition** or **metallicity**. Pop I stars formed more recently than Pop II stars. In reality there is a continuous spread of age, of course, and hence a continuum of

SECTION 1 - INTRODUCTION

population characteristics, giving rise to terms such as **extreme Pop I**, intermediate Population between I and II, and **extreme Pop II**.

The first generation of stars born after the Galaxy itself was formed, would have had **near-primordial composition** of elements, *i.e.* their relative amounts of hydrogen and helium (and essentially nothing else) were as formed in the late stages of the Big Bang by **nucleosynthesis**. We can state this because the ages of the oldest stars in the Galaxy (in globular clusters) are not much less than the currently estimated age of the Universe, which is approximately 13 billion years. Most of the elements heavier than helium are only produced in supernovae. Hence, later generations of stars are born from interstellar clouds which are enriched by these heavy elements. See below for further discussion of stellar life cycles and Galactic history.

Thus, Pop I stars have a higher proportion of heavy elements than Pop II stars have. In fact, for some years astronomers have searched for evidence of surviving members of the original generation of stars, **Pop III stars**, which would be the oldest stars in the Galaxy and would have chemical compositions matching those calculated to have been produced from the Big Bang.

Definitions of metallicity, [Fe/H], X,Y,Z

Astrophysicists commonly use the symbols (X,Y,Z) to refer to the chemical composition of stars, or of regions within stars, or other objects. These are defined to be the **fractional abundance** of hydrogen (X), helium (Y), and all others (Z). These fractions are normally calculated in terms of the **relative mass** of hydrogen *etc.* present, rather than by the relative number of atoms present. Note that:

$$X + Y + Z = 1$$

Equation 1.1

The 'all other' elements, *i.e.* all elements more massive than helium, are usually referred to as **heavy elements** or **metals**. The latter term is very misleading since of course only some of these elements are metals in the normal scientific sense of the word. Indeed, carbon and oxygen for example are some of the most common elements in the Universe after hydrogen and helium, and they are certainly not metals. However, astronomers continue to use this term, and you will see it in many astrophysics texts and papers. The main reason for this usage is that the value of Z is frequently estimated by analysis of stellar spectra in which lines of iron, magnesium and other real metals are the easiest to measure and interpret. An example of this usage appears in our list of components of the Galaxy above, where we mention the metal-poor halo and the metal-rich halo. The former has Z substantially lower than the latter.






- For the Sun's photosphere, the values of (X,Y,Z) are approximately (0.70, 0.28, 0.02).
- For extreme Pop I stars, Z can be 0.04 or more. For extreme Pop II stars, Z can be as low as 10^{-5} .

The abundances of heavy elements are also commonly specified in the following way. Suppose that the relative number of atoms of element Q compared with

The Solar Neighbourhood

Our local spiral arm contains most of the well-known naked-eye objects and those seen through a small telescope. By far the most common stars are dim red dwarfs, but the main contributors to the optical starlight are hot stars. The local interstellar medium consists of small cold clouds and warm tenuous regions immersed in a bubble of hot plasma. In this Section we investigate the stellar and interstellar components of the solar neighbourhood.

The local spiral arm

ICON KEY	
	Valuable information
	Test yourself
	Worked example
	Textbook
	Important Equation

Our spiral arm is a **region of enhanced density** within the thin disc of the Galaxy. It is some 1000 pc wide within the plane and about 500 pc thick. The Sun is just 15 pc above the midplane of the disc, *i.e.* $z_{\odot} = +15$ pc.

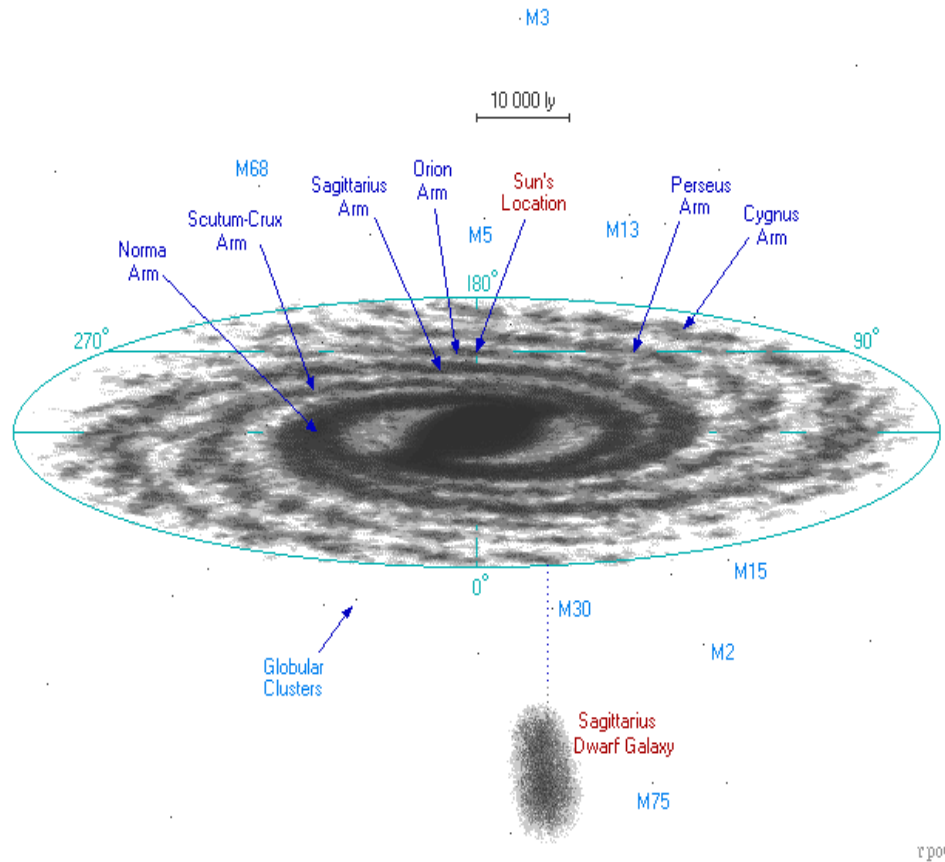
We start this Section by looking at the **distributions of stars and stellar types** in the local spiral arm within a few hundred parsecs of the Sun. Then we zoom in to specifically consider our closest neighbours – those within only a few parsecs of us. Finally, we investigate the content and physical conditions of the **interstellar medium (ISM)** in the solar neighbourhood. Within this framework, we will also introduce important concepts of wider significance, such as stellar mass functions, distance determinations and the techniques of absorption line spectroscopy.

In conjunction with this Section of Notes, you should read Sections 2.1, 2.2.1 and 2.2.2 of *Sparke & Gallagher*. In particular, this includes further discussion of stellar luminosity functions and stellar mass functions.

Our local spiral arm is often called the **Orion arm**, or the Orion-Cygnus arm. Within the arm and approximately in the direction of the Galactic anti-centre lie many of the stars in the constellation of Orion. In fact, the brightest early-type (O,B,A type) Orion stars are part of a co-moving group called Gould's Belt (see below) which is a young group forming a rough disc shape, tilted at an angle of about 20° to the plane. These Orion stars are up to $b \sim 20^{\circ}$ ($z \sim 200$ pc) *below* the plane in the direction $l \sim 200^{\circ}$. In addition, *along* the local arm in the direction $l \sim 80^{\circ}$ lie many of the stars in the constellation of Cygnus.



Figure 2.1. Sketch view (negative) of the Galaxy showing the location of the local (Orion) arm and other spiral arms. Image by Richard Powell (See: <http://www.answers.org/free/universe/index.html>)



r powell

Figure 2.2. A Schmidt telescope image of a star field in Cygnus and the western part of the Cygnus Loop supernova remnant. This image covers just over one degree square on the sky, looking along the local arm towards $l \sim 80^\circ$, $b \sim -8^\circ$. The Cygnus Loop is at a distance of ~ 800 pc. The bright foreground star is 52 Cyg. Image: N.A.Sharp, REUprogram/NOAO/ AURA/NSF. (See:http://www.noao.edu/image_gallery/html/im0533.html)



The Sun lies on the Galactic-centre side of the local arm, about 500 pc from its **central ridge-line**, which is delineated by concentrations of young open clusters and star-formation regions. The adjacent **Sagittarius-Carina spiral arm** lies closer to the Galactic centre than the local arm, whilst the **Perseus arm** is the next one in

A common situation in which such an absorption spectrum arises is when the **cooler atmosphere of a star** is absorbing some specific wavelengths of the continuous emission spectrum, which is itself coming from the hotter lower layers of the stellar photosphere. Then the illustrated form of spectrum output would occur if the input source were the image of the star trailed along the slit. The result is a **continuous spectrum** with **absorption lines** superimposed on it.

However, in the present context, imagine this source is the trailed image of a star which happens to be behind a cloud of **cold interstellar gas**. The output spectrum will contain absorption lines from the stellar atmosphere, but also might contain some other absorption lines, the latter due to absorption by atoms in the interstellar gas which happens to be in the line of sight to the star.

Discovery of interstellar gas

Interstellar gas atoms and ions were discovered in the early years of the 20th century. In 1904, Hartmann discovered interstellar Ca^+ in the line of sight to the star δ Orionis. This was followed by a series of discoveries over the next 50 years in the optical part of the spectrum, and subsequently continued with many discoveries in the ultraviolet with the three space telescopes *Copernicus*, *IUE* and *HST*, in the last 30 years of the 20th century.

The **name given to the spectrum** of the ion Ca^+ is Ca II. The spectrum of the neutral Ca atom is called Ca I, and that of the doubly ionised Ca^{++} is Ca III, and so on. The Fe XV spectrum comes from the ion Fe^{14+} which is formed at over 10^6 degrees (as in the example of the solar corona shown in Figure 2.12 above).

Hartmann had found the strongest optical interstellar absorption lines, namely those designated the **Ca II H and K lines**. Now, you need to note that these *H* and *K* lines are nothing to do with the elements hydrogen and potassium. They are just the original Fraunhofer (1815) labels for the strongest lines in the solar visible spectrum, and astronomers still use these labels today. (See Section 1.1.2 of *S&G*.) They are in the violet part of the spectrum at wavelengths 393.4 and 396.8 nm. The second strongest lines seen were in the yellow: the **Na I (sodium) D lines** at 589.0 and 589.6 nm. Other optical interstellar spectra identified included Ca I, K I, Ti II, Fe I, and the diatomic species CH, CH^+ and CN.

There is a fascinating additional twist to the story of these discoveries. Those observations of the species CH, CH^+ and CN indicated two separate physical conclusions. First, since they are not stable species in laboratories on Earth and can only exist for any length of time in very low density environments, the interstellar gas must be of **very low density**. Secondly, observations made by McKellar in 1941 of the ratio of intensities of two CN lines (and hence of the excitation temperature of the species) showed that the interstellar gas was bathed in a pervasive ambient temperature of 2.3 K. Re-calculations of this using the best modern data yield between 2.7 and 2.9 K. This should have been the discovery of the **cosmic microwave background**, but instead these observations were completely incomprehensible to theorists at the time. The data were then largely forgotten for 25 years, and only remembered after the much-more-famous Penzias and Wilson serendipitous microwave observations in 1965.

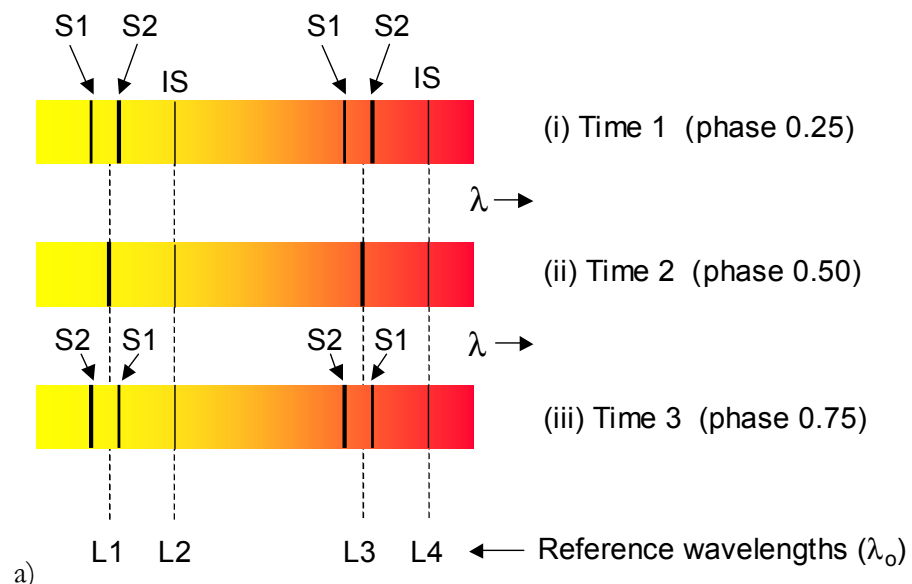
The **ultraviolet region** of the spectrum contains a much richer selection of interstellar lines. Most of the strongest absorption lines are in the UV. This is because the atoms are normally in their **lowest energy state** in the rarefied interstellar gas, and the transition from there to the next state is a large one. Such a large energy change corresponds to a high frequency and a short wavelength of radiation. A simple example is found in hydrogen (see *University Certificate in Astronomy* notes chapter 5, and *Universe* chapter 5). Here, the Lyman series of UV absorption lines corresponds to transitions from level 1 to level 2 (Lyman α), from level 1 to level 3 (Lyman β), and so on. UV interstellar spectra include H I, C I, C II, C III, C IV, N I, N II, N V, O I, O VI, Mg I, Mg II, and many others.

In the low densities of interstellar space, the atoms rarely undergo collisions and so their electrons spontaneously cascade down into the lowest energy configurations. Thus normally it will be the lowest energy state (ground state) of the atoms that will be most populated. When such an atom encounters an ultraviolet photon of the right frequency, it will absorb it, moving one of its electrons from the lowest to a higher energy state. Hence, UV photons from a star in the line of sight of an observer can be absorbed by interstellar gas, and the evidence for this is the presence of UV interstellar absorption lines in the spectrum of that star.

Stationary lines in the spectrum of spectroscopic binaries

Hartmann's original discovery was based on observing the behaviour of the spectrum of certain spectroscopic-binary stars including δ Ori. Whereas the absorption lines produced in the stellar spectrum move back and forth in wavelength with a regular periodicity, due to the Doppler shifting of lines from the moving stars in the binary, on the contrary some other lines stayed stationary. It was soon realised that these **stationary lines** must be due to interstellar gas in the line of sight, somewhere between the binary system and the Earth.

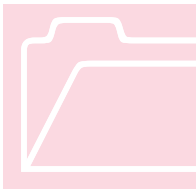
Figure 2.14 (a) Series of spectra of a spectroscopic binary (SB2) system at 3 different phases of the binary. Absorption lines L1 and L3 arise in the stellar atmospheres within the fast-rotating binary system, and move back and forth due to the Doppler effect, causing redshifting and blueshifting of the spectral lines. Lines L2 and L4, on the other hand, arise from the interstellar gas which is at approximately constant velocity relative to the observer.



other internal forces continues throughout the whole life of a star. These internal forces derive from ideal-gas pressure, radiation pressure or degeneracy pressure, and from factors such as high stellar rotation or strong magnetic fields. Recall, in particular, that if a main-sequence star's temperature rises, its (ideal-gas) pressure rises and this will oppose gravitational contraction.

For a star on the main sequence, the two opposing forces are locked in a stalemate (*i.e.* the detailed balance of **hydrostatic equilibrium**, *University Certificate in Astronomy Notes* Section 8). Later in a star's life, internal pressure may win temporarily, as in the expansion to a red giant stage, and gravity may win for a while, as when the star contracts to a white dwarf – until the electron-degeneracy-pressure sets in and holds gravity at bay. At the end of the day, the gravity/pressure battle for very-high-mass stars, for example, results in spoils for both sides – a supernova explosion and a remnant black hole.

This battle – the balance between these opposing forces – is encapsulated in one of the most powerful and far-reaching statements in the whole of physics and astronomy. The statement is elegant and startlingly concise. It is the **Virial Theorem**.



The Virial Theorem has very important applications in the study of all stages of a star's life, of molecular clouds and star formation, and of stellar clusters, galaxies, and clusters of galaxies. Indeed, the theorem has wide applications in physics in general and thermodynamics in particular. Here, the Virial Theorem will enable us to calculate the minimum mass of cloud that will collapse to form a star. This limiting mass is called the **Jeans Mass**, named after Sir James Jeans.

The Virial Theorem and the Jeans Mass

The Virial Theorem tells us how to combine the various kinetic energy sources and potential energy sources within a particular physical system (say, a molecular cloud, or a large star cluster), in order to deduce whether the system is stable or will expand or will collapse.

Historical development

The theorem is deceptively simple in form, and has in fact been developed, studied and used for over 200 years. It is based on an essay published by Lagrange in Paris in 1772 which included a concept subsequently known as **Lagrange's Identity**. Two other very famous scientists, Jacobi (from 1842) and Clausius (from 1870), generalised it to many-body systems (**n-body systems**).

In astrophysics, the n bodies may be either the **molecules in a molecular cloud**, or the ions and electrons in a star, or the **stars in a star-cluster**, or even the galaxies in a galaxy-cluster. Strictly speaking, the theorem is only accurate if the number of such bodies is *very* large (as is certainly true in the case of molecules in a molecular cloud). However, it can also be applied (with care) to systems with relatively small numbers of bodies, such as the stars in stellar clusters (see Section 4 of these Notes for examples of this).

It was Clausius who coined the term 'virial', stating that "the mean *vis viva* of the system is equal to its *virial*" when it is stable (quoted by G.W. Collins in his

monograph entitled ‘The Virial Theorem in Stellar Astrophysics’, Pachart, 1978). Here, the *vis viva* (“life-force”) is what we call *kinetic* energy, and the *virial* is also derived from the Latin for “forces”. The *virial* equates to *half* the average *potential* energy.

Thus the modern form of the **Virial Theorem for stable closed systems** is:

$$2 KE + PE = 0 \quad \text{Equation 3.3}$$

where *KE* is the total kinetic energy, and *PE* is the total potential energy of the system.

Whilst a proof of the theorem is beyond the scope of this course, if you are interested in seeing one type of proof which starts from Newton’s law of gravity, this can be found in *S&G* section 3.1, leading to equations 3.40 and 3.42. It is important that you understand that the number 2 appearing in the Virial Theorem is **exactly 2**. Note that the *PE* term is negative: gravitational potential energy is always negative. The *KE* term is, of course, positive.

Equation 3.40 in *S&G* shows a form of the equation which also includes (a) a term for the work done by forces external to the system (such as those which may trigger the onset of cloud collapse) and (b) a term involving the moment of inertia of the system which allows for the more general cases of contraction and expansions as well as stable equilibrium.

For a star or cloud in **equilibrium**, and where the only significant contribution to potential energy is the **gravitational potential energy**, Ω , and where the only significant contribution to kinetic energy is the **internal thermal energy**, \mathfrak{S} , we obtain the simplest form of the Virial Theorem:

Simplest form

$$2 \mathfrak{S} + \Omega = 0 \quad \text{Equation 3.4}$$

In general, however, it is necessary to add other terms in this equation. These will include the kinetic energy of **turbulent motion**, Φ and of **rotation** \mathfrak{R} , of the system (*e.g.* rotation of the molecular cloud as a whole), and also **magnetic potential energy**, U_m . All of these are positive quantities; all these effects oppose gravity. Then the equation becomes:

System stable against collapse

$$2 \mathfrak{S} + 2 \mathfrak{R} + 2 \Phi + U_m + \Omega = 0 \quad \text{Equation 3.5}$$

Furthermore, if the system is in accelerative expansion, rather than in stable equilibrium, the right-hand-side will be a positive quantity rather than zero. This is because the sum total of all the positive terms, *i.e.* everything except gravity, exceeds the modulus of the negative term (gravity).

System unstable to collapse

If, however, the system is **unstable to collapse**, then gravity is dominating all the other terms combined, and in this case the right-hand-side is negative:

$$2 KE + PE < 0 \quad \text{Equation 3.6}$$

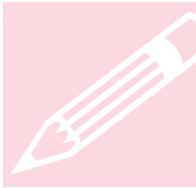
Equation 3.6 describes the case where gravity is winning the battle; and equation 3.5, the case where all the energies of rotation, heat, turbulence and magnetism are pitted against gravity and there is stalemate – the system is stable against collapse or expansion.

There is a very important corollary to the simplified Virial Theorem (equation 3.4). If a cloud slowly contracts, such that at each moment it is almost in equilibrium, and equation 3.5 applies to small changes in the energies, it is called a **quasi-static contraction**. In this case, the same equation gives:

$$\Delta\mathfrak{S} = -\Delta\Omega / 2 \quad \text{Equation 3.7}$$

Thus, the change (increase) in the internal thermal energy is equal to half the change in the gravitational energy of the system. As the system contracts, half the gravitational energy released in the contraction goes into heating the cloud. The other half goes elsewhere – normally it is radiated away, as increased luminosity.

Using simple formulae for the gravitational and thermal energies, we can calculate the change in temperature of the cloud, and also its luminosity. For a protostar this will show us its change of location on the HR diagram.



Worked example. A $1M_{\odot}$ protostar of uniform density contracts quasi-statically from a radius of $120R_{\odot}$ to $100R_{\odot}$ in 100 years. Assuming the simplified Virial Theorem applies, calculate (a) the gravitational potential energy released; (b) the increase in its internal mean temperature; (c) its average luminosity during this period if this solely arises from the release of gravitational energy. The gravitational potential of a uniform sphere is given by

$$\Omega = \frac{-3}{5} \frac{GM^2}{R} \quad \text{Equation 3.8}$$

The thermal energy is given by:

$$\mathfrak{S} = \frac{3kT}{2} \times (\text{total number of particles}) = \frac{3kT}{2} \times \left(\frac{M}{\mu m_H} \right)$$

$$\text{Equation 3.9}$$

and you may assume that $\mu = 1.0$.

(a) First calculate the gravitational energy released. This is equal to

$$\begin{aligned} \Delta\Omega &= \frac{-3}{5} GM^2 \left(\frac{1}{R_2} - \frac{1}{R_1} \right) \\ &= -1.58395 \times 10^{50} \times \frac{1}{6.96 \times 10^8} \times \left(\frac{1}{100} - \frac{1}{120} \right) \\ &= -3.792 \times 10^{38} J \end{aligned}$$

(b) From equation 3.7, half this is converted into thermal energy, so that

$$\Delta\mathcal{S} = 1.896 \times 10^{38} \text{ J} \quad \text{and so the rise in mean temperature is:}$$

$$\Delta T = \Delta\mathcal{S} \times \frac{2\mu m_H}{3kM} \quad \text{and } \mu = 1. \quad \text{Hence,}$$

$$\underline{\Delta T = 7700\text{K}}$$

(c) Average luminosity = (half the released gravitational energy)/(100 years)

$$= (1.896 \times 10^{38} \text{ J}) / (100 \times 3.156 \times 10^7 \text{ s})$$

$$= \underline{6.01 \times 10^{28} \text{ W} = 156 L_{\odot}}$$

Note that its position in the HR diagram will be near the top of the Hayashi Track. (Assuming a black body we can use $L = 4 \pi R^2 \times \sigma T^4$ for $R = 100 R_{\odot}$ and $L = 156 L_{\odot}$ and so $T_{\text{eff}} = 0.35 T_{\text{eff}\odot} = 2040 \text{ K}$.)

Jeans Mass

Considering equation 3.6, and assuming that the dominant terms are thermal kinetic energy and gravitational potential energy (as in equation 3.4), we can calculate a **critical mass** of the molecular cloud, above which it will become unstable to collapse. This critical mass, the minimum mass for the cloud to collapse towards formation of stars, is called the **Jeans Mass**, as mentioned above.

From equation 3.6, the condition for collapse to start is

$$2\mathcal{S} < |\Omega|$$

and hence:

$$\frac{3MkT}{\mu m_H} < \frac{3GM^2}{5R} \quad \text{Equation 3.10}$$

By expressing the radius R in terms of the mass and density, this can be seen to give a formula for the critical mass, above which collapse would take place. A more detailed derivation yields the **Jeans Mass** for this critical mass, M_J .

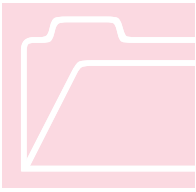
$$M_J = \left(\frac{\pi k T}{\mu m_H G} \right)^{3/2} \times \rho^{-1/2} \quad \text{Equation 3.11}$$

$$\cong 2 \times 10^4 \times \sqrt{\frac{T^3}{n}}$$

where n is the number of particles m^{-3} and the result is expressed in units of solar mass. (Note however that if you are using the full expression, *i.e.* the first

Self Test Questions on Section 3

1. What are the main constituents of molecular clouds? Why is the gas in these clouds in molecular form?
2. Compile a Table which summarises the similarities and differences between Giant and Dwarf Molecular Clouds.
3. Explain in your own words the meanings of the terms (a) recombination lines, and (b) forbidden lines.
4. Calculate the gravitational potential energy (in Joules) of a uniform density sphere with mass $5 \mathcal{M}_{\odot}$ and radius equal to the size of Neptune's orbit.
5. Calculate the thermal energy in a $1 \mathcal{M}_{\odot}$ cloud of pure molecular hydrogen at a temperature of 10K.
6. A molecular cloud of uniform density contracts quasi-statically from a very large radius to a radius of 0.1 AU. Its internal mean temperature rises to 1000K in this time. What is the mass of the cloud?
7. Calculate the Jeans Mass for a cloud with density 10^{10} particles m^{-3} and temperature of 300K.
8. A $1000 \mathcal{M}_{\odot}$ cloud is supported only by thermal kinetic energy. The temperature decreases to 100K and the density increases to 10^8 molecules m^{-3} . Will it collapse under its own gravity?
9. Explain why astronomers are convinced that only low-mass stars are born in globules (dwarf molecular clouds).
10. What is the strongest evidence for the presence of bipolar outflows from young stars, in your opinion?
11. Why are emission lines from neutral hydrogen (H I) dominant in an H II region? Why is it not called an H I region?
12. Write a short account of the birth, life and death of a T Tau star.



Distribution of open clusters

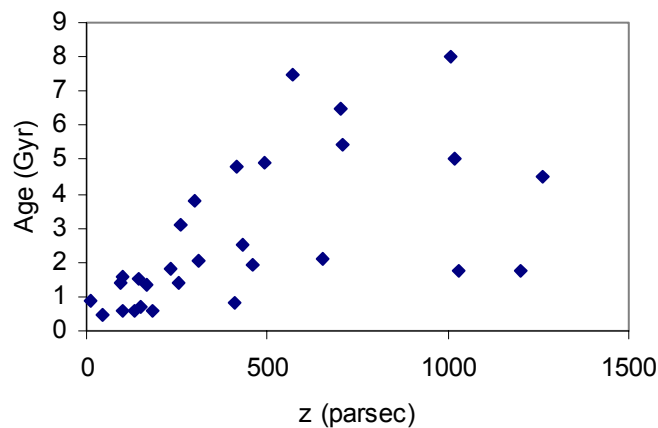
Open clusters tend to lie in, or close to the plane of the Galaxy, near to where they were born. Older open clusters are rare, but lie preferentially away from dense regions of the disc, further out in the Galaxy and away from the Galactic disc (as seen for a sample of clusters plotted in Figure 4.8). Old clusters are not detected in the Galactic plane (within a few hundred parsecs above or below the plane). Recall that the disc scale height is about 200 parsecs for young stars. In the plane, the damaging effects of gravitational perturbations from the disc and giant molecular clouds easily disrupt loosely bound open clusters, so the only ones we see are the younger ones.

There is also a decrease in the metallicity of open clusters with distance from the centre of the Galaxy. This follows the decrease of metallicity seen also in the disc stars and in the ISM. This gradient of metallicity implies that there has been less recycling of stars further out in the disc and supports the idea that the star formation rate decreases where the ISM gas density is lower.

Figure 4.8

A plot of the location of older open clusters relative to the plane of the Milky Way. Here z is the vertical distance from the Galactic plane.

Data from Carraro & Chiosi 1994, A&A, 287, 761



Let us look now at some of the dynamical timescales and dynamical processes that determine the evolution of star clusters.

Dynamical evolution of star clusters

Why do some open clusters survive longer than others? This depends partly on where the stars formed and the external gravitational perturbations due to molecular clouds etc.. The longevity of an open cluster also increases with the number of stars and compactness of a cluster, as these factors increase the self-gravity of the cluster and the depth of its **gravitational potential well**. Open clusters containing thousands of stars are more likely to survive disruptions than clusters containing only a few tens of stars.

There are many more young open clusters than old ones in the Galaxy. This scarcity of old open clusters is a consequence of the easy destruction of such clusters by interactions with molecular clouds in the disc. The older open clusters tend to survive longer in less hostile regions, slightly further from the Galactic plane and/or further from the Galactic Centre. Those most vulnerable to destruction are the poorly populated, less centrally concentrated open clusters, near

to the Galactic disc and closer to the Galactic centre. Therefore we do not see any old versions of these types of clusters.

Equipartition



Within open clusters, the gravitational interactions of the stars will tend to share (i.e. **partition**) their energies equally amongst the stars of different masses. This is known as **equipartition of energy** and, in practice this means that the stars have similar **kinetic energy** (KE). The KE of a star of mass m moving with velocity v is:

$$KE = \frac{mv^2}{2} \quad \text{Equation 4.4}$$

Therefore for KE to be equally partitioned amongst the stars, more **massive stars** will move more **slowly**. This results in more massive stars congregating more centrally and less massive stars tending to be found further out in star clusters. This is called **mass segregation**. As a consequence less massive stars are more likely to be lost from the cluster. Near the extremes of their orbits they only need a small kick to escape the weak gravitational potential at the outskirts of the cluster. Such a gradual loss of stars from a cluster is known as **evaporation**. Thus the mass function of stars in a cluster may be biased towards more massive stars, if there has been enough time for significant preferential evaporation of the less massive stars to take place.

Relaxation



The equipartition of energy occurs on a timescale known as the **relaxation time**. Each star gradually changes its velocity (both its speed and direction) due to long-range interactions with gravitational fields of other stars in the system. The relaxation time, t_{relax} , increases with the number of stars, N , in the system such that:

$$t_{relax} = \frac{N \times t_{cross}}{6 \times \ln(N/2)} \quad \text{Equation 4.5}$$

where t_{cross} , the **crossing time**, is the time it takes a star to cross the cluster. Proof of Equation 4.5 goes beyond the scope of this course, but, for the interested reader, it can be found in *SciG*, section 3.2.2. Equation 4.5 tells us that less numerous star systems take a shorter time to relax to energy equipartition. The crossing time is $t_{cross} \approx R/v$, where R is the radius of the cluster. The velocities of stars in an open cluster are typically $\sim 1 \text{ km s}^{-1}$.

As an example, the Hyades is about $1.5 \times 10^{14} \text{ km}$ across, so its crossing time is about 2×10^6 years, and its relaxation time is about 1×10^7 years. Since the Hyades is much older than this (see Table 4.2) the cluster should, if left to itself, have relaxed to a symmetric shape. However, the Hyades is an irregularly shaped cluster, which implies that external forces have distorted it.



Globular clusters

There are about 160 **globular clusters** in our Galaxy and they contain some of its oldest stars. They are relaxed, almost spherical distributions of a few million stars, several parsecs across, with compact cores of radii ~ 1 parsec. Their compactness

helps them to survive against disruption by external gravitational perturbations. The stars in globular clusters are generally metal-poor compared to the Sun.

You should now read section 2.2.3 of *S & G*, which discusses some aspects of star clusters. For confident readers who seek a more advanced (level 3) treatment, chapter 6 of *Binney & Merrifield* gives a much more comprehensive, in-depth overview of both globular and open clusters.

Distribution in the Galaxy

The system of globular clusters is distributed throughout the visible halo of our Galaxy, filling a roughly spherical volume. It rotates slowly compared with the disc. It is supported against collapse under gravity by the kinetic energy associated with the velocity dispersion of globular clusters. Globular clusters move at speeds of $\sim 200 \text{ km s}^{-1}$ on **orbits inclined to the Galactic plane**. More metal-rich globulars tend to congregate closer to the Galactic plane, as Figure 4.9 shows.

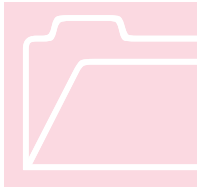
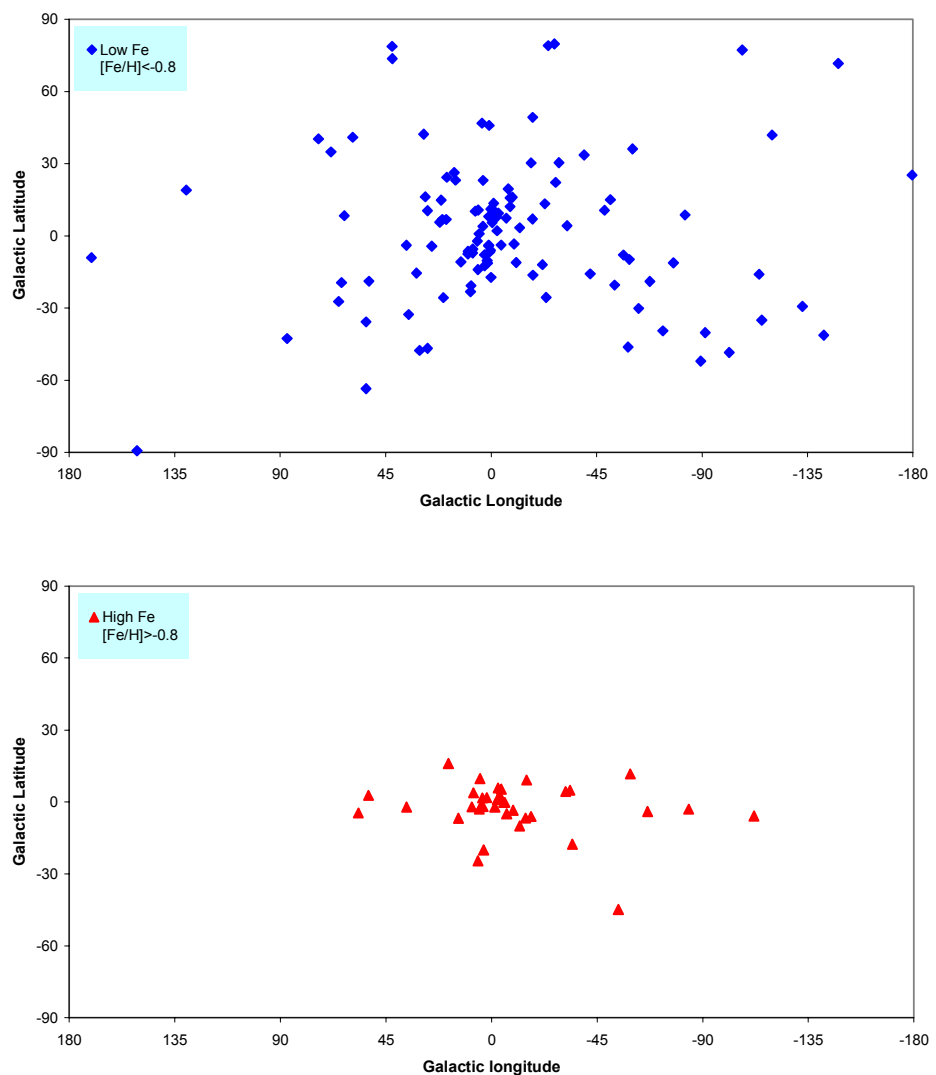


Figure 4.9
 Distribution (in Galactic coordinates) of globular clusters in our Galaxy:
 Top) metal-poor ($[\text{Fe}/\text{H}] < -0.8$)
 Bottom) metal rich ($[\text{Fe}/\text{H}] > -0.8$) globulars. The Galactic centre is in the middle of each image, as observed from the Sun.

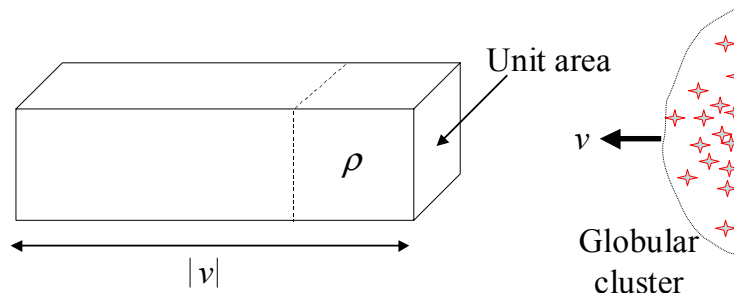


An example of a globular cluster is present in Figure 4.5. Check that you can recognise it, to the lower right in this image. See also Figure 1.2 for another example of a globular cluster.

Ram pressure

Globulars contain very little gas, since this would be easily removed by the ISM when the clusters traverse the Galactic disc. The main gas removal mechanism is via **ram-pressure stripping**. In this process gas in a globular is forced out by the pressure of the gas in the ISM acting on it.

Figure 4.10
Illustration of the volume of ISM gas (density ρ) traversed per unit time by a globular cluster moving with velocity v relative to the ISM.



Consider a globular cluster moving at a constant velocity v relative to the ISM of density ρ . Then the mass of ISM hitting the globular per unit time, per unit area is:

$$\text{Mass per unit time crossing unit area} = \frac{dM}{dt} \text{ per unit area} = \rho v$$

If we multiply $\frac{dM}{dt}$ by the constant velocity v , we obtain the *rate of change of momentum per unit area*, which we know from **Newton's second law** to be a force per unit area, *i.e.* a pressure. The force F_{ISM} exerted by this gas flow is:

$$F_{ISM} = \frac{d(Mv)}{dt} = v \frac{dM}{dt} \quad \text{since } v \text{ is a constant.}$$

Since pressure is force per unit area, the ram-pressure P must be F_{ISM} per unit area:

$$\text{ie } P = \left(\frac{dM}{dt} \text{ per unit area} \right) \times v = (\rho v) \times v = \rho v^2 .$$

For this ram-pressure to be sufficient to remove the gas (of density ρ_{gas}) from the globular cluster the following must be true:

$$P = \rho v^2 > \frac{\sigma^2 \rho_{gas}}{3} \quad \text{Equation 4.6}$$

Here σ is the **velocity dispersion** of the stars in the globular cluster and is related to the depth of the gravitational potential well due the mass in the globular cluster. The **Virial theorem**, that we met in Section 3, relates the kinetic energy KE and potential energy PE of a system in dynamical equilibrium:



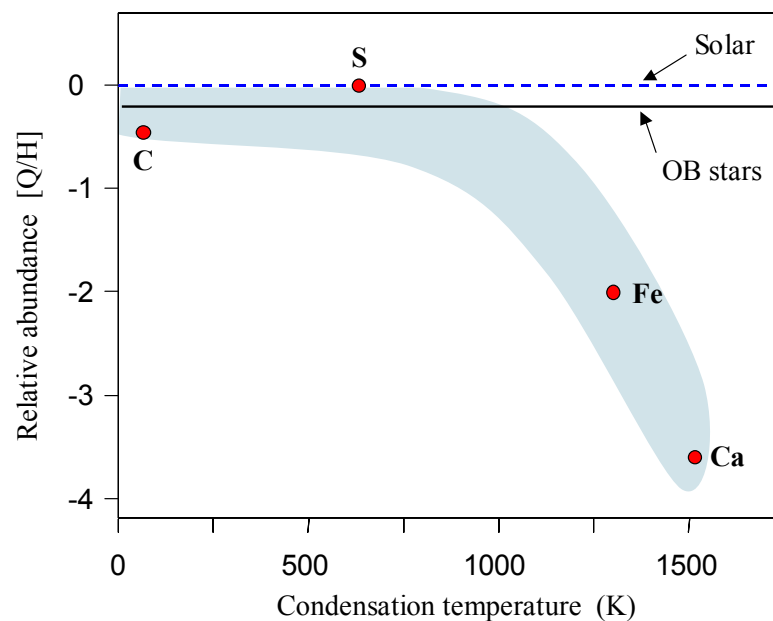
Note that the derivation of the inequality shown in Equation 4.6 comes from a treatment more advanced than is required for this course.

Interstellar gas depletions

Amongst the first evidence for the presence of certain elements in grains was that from **interstellar gas depletions**. As we discussed at some length in Section 2 of these *Notes*, there is a well-established method for determining the abundances of the elements in interstellar gas. It involves measuring the equivalent widths of absorption lines and calculating **column densities** N , of the various gas species. When looking along sightlines through substantial quantities of dust, some elements have lower abundances than normal but others are unaffected. The obvious conclusion is that the amounts of these elements missing from the gas phase are instead present in the dust within the same clouds. The most important data contributing to these studies came from observations in the UV, with the satellites *Copernicus*, *International Ultraviolet Explorer (IUE)* and *Hubble Space Telescope (HST)*.

A schematic summary of these depletions for typical sightlines through diffuse clouds, is shown in Figure 5.6.

Figure 5.6. Schematic diagram indicating the depletion of elements from the interstellar gas phase to dust grains. Gas-phase abundances relative to solar values, are shown plotted against the condensation temperature of the elements.



The interstellar gas depletion is defined to be the relative abundance

$$[Q/H] = \log_{10} (N_Q/N_H)_{\text{gas}} - \log_{10} (N_Q/N_H)_{\odot} \quad \text{Equation 5.13}$$

which is analogous to Equation 1.2 from Section 1 of these *Notes*, and where the solar-system abundances represent the overall ISM total abundances. (Alternatively, the depletions are sometimes calculated relative to the mean OB stellar (extreme Population I) abundances – see Figure 5.6.)

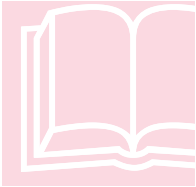
Thus, if the depletion is zero, all of the element is in the gas. If it is -1 , then 10% of the element is in the gas and 90% is in dust. If it is -2 , then 99% is in dust and only 1% remains in the gas phase.

SECTION 5 - INTERSTELLAR DUST

Figure 5.6 indicates these depletions plotted against the **condensation temperature** of the various elements, because it was found that these seem to be related, perhaps giving clues to the temperatures of formation and processes of formation of dust grains. **Volatile elements** such as carbon, nitrogen, oxygen, sulphur and zinc are *lightly* depleted. More **refractory elements** such as silicon, iron and calcium are more *heavily* depleted.

This result was first shown in a famous paper by Field published in the *Astrophysical Journal* in 1974.

Depletions of many elements, such as calcium for example, are correlated with the mean space density along the sightline, as first shown by Harris and Bromage in 1983: this indicates that atoms are exchanged between dust and gas depending on the environmental conditions.



We can group the elements into three categories (as discussed in detail by Whittet, D.C.B., *Dust in the Galactic environment*, IoP, 2003):

- Elements which have **low depletions** in all environments, including C,N,O,S and Zn, and in terms of overall abundances these are dominated by C and O;
- Elements with **intermediate depletions**, low in the intercloud medium and high in clouds. This category is dominated by Mg and Si but also includes P; these elements can be considered to be “migratory” between the gas and the grains; and
- Elements that have **high depletions** in all environments, hinting that these form a near-indestructible grain material. The depletions are correlated with the mean ISM density along the sightline. This category is dominated by Fe in terms of overall abundances, and also includes Ti, Ca, Cr, Mn and Ni.

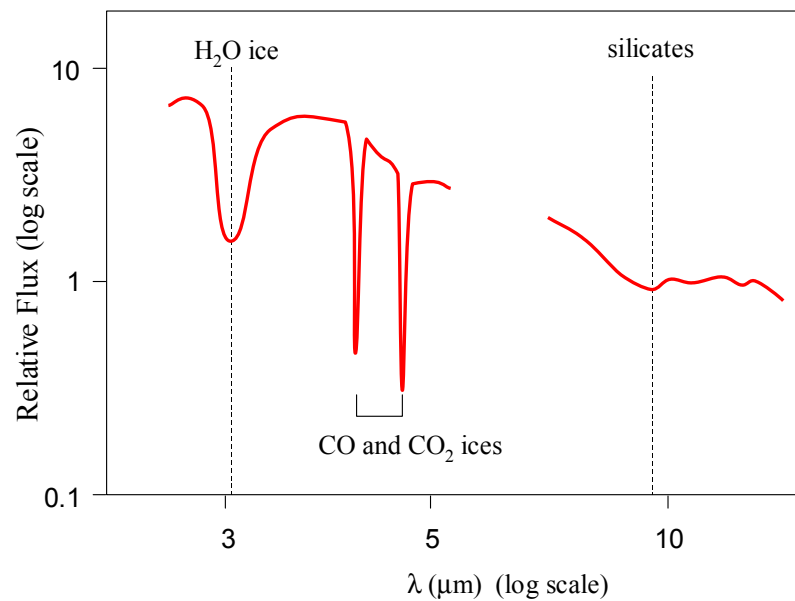
Grain Composition

There are specific **spectral features in the infrared** which strongly indicate the presence of certain grain materials. These include various ices (H₂O, CO, CO₂ and others) and silicates. See Figure 5.7.

Considering now the sum total of observational constraints, we must note the depletions, the clues from the infrared spectra, and the possible models that will match the interstellar extinction and polarisation observations. Thus,

“Models for interstellar extinction must explain the observed opacity per H atom and its wavelength dependence, without exceeding the quota of available elements set by the abundances and depletions.” (Whittet, op. cit. p.64).

Figure 5.7. Schematic depiction of the infrared spectrum of a heavily-reddened star behind the Taurus dark molecular cloud. The absorption features include ones identified with H₂O ice, CO and CO₂ ices, and silicates.



Conclusions

Scattering and polarisation data point to at least one major component being of dielectric material and the grains being relatively large. The extinction and other evidence points to needing a combination of relatively large (classical) grains and some small grains needed to explain the far-UV rise in the extinction curve. Most of the mass must be in the larger grains. The material may well include very porous aggregate grains, since this would probably optimise the extinction per unit mass.

A substantial contribution is needed from C-rich grains as well as O-rich grains, in order to fully explain both the opacity of dust per H atom and the 220nm feature (Figure 5.5). These refractory particles must acquire icy mantles, at least temporarily, whilst they are inside cold dense interstellar molecular clouds.

The infrared spectra favour silicates (Si+O) rather than silicon carbide (Si+C). The most likely silicates are those containing magnesium, since Mg and Si appear to have the same depletion behaviour (see above). These could well include MgSiO₃ (pyroxene type) and Mg₂SiO₄ (olivine type).

Role of dust in the life cycle of stars

Interstellar dust is intimately involved in the formation and evolution of stars and of planets. Dust probably plays an important role in almost all phases of the life cycle of stars.

Production of grains in stellar atmospheres, and stellar mass loss

In the post-main-sequence phases of stellar evolution, there are episodes of considerable mass loss, especially during the red giant and red supergiant phases. The **mass-loss rates** in oxygen-rich red giants are 10⁻⁸ to 10⁻⁷ M_⊙ yr⁻¹. For red supergiants they can be 10⁻⁶ to 10⁻⁵ M_⊙ yr⁻¹. Such evolved stars are sources of the production of interstellar grains, although they may subsequently grow mantles of volatile materials in cold interstellar clouds.

The spectra of oxygen-rich atmospheres of evolved stars show infrared features in emission which are identified with **amorphous silicates**. These features are very





The Radio Galaxy and Spiral Arms


Until the advent of radio astronomy in the 1930s our study of the Galaxy was restricted to those regions not obscured by interstellar dust. From the beginning the Galaxy featured as a prominent contributor to the radio sky. The long wavelength of radio photons allows them to penetrate interstellar dust, and so radio astronomy gave us our first tool for examining the entire Galaxy. From observations of hydrogen and other radio-emitting species we have established the two-armed spiral structure of our home “city of stars” and along the way constrained how the spiral structure has formed and is maintained.


The Galaxy at radio wavelengths


ICON KEY

 Valuable information

 Test yourself

 Worked example

 Textbook

 Important Equation

One of the great surprises of twentieth century astronomy was the discovery of emission of extraterrestrial origin at radio wavelengths. When Karl Jansky set up his antenna array in 1931, he was investigating static from thunderstorms in order to improve radio communications. Almost as a footnote to his first findings was the discovery of “...a steady hiss type static of unknown origin.” By 1933 he was convinced that this emission originated outside the solar system, and by 1935 he was confident that the dominant component came from the **Milky Way**. Indeed even in a plot of the intensity of this static by Jansky in 1932, the radio emission peak towards the **Galactic centre** is clearly visible. Since that time radio astronomy has rapidly assumed great importance, allowing the discovery of new types of astronomical objects (e.g. pulsars, quasars) and the observation of the most distant regions of our Universe.

As a historical note, radio astronomy was the first of the **new astronomies** of the twentieth century – astronomical techniques operating outside the visual band to which astronomers had previously been restricted. In addition to new discoveries, these techniques required new approaches, such as accurate automatic pointing of telescopes (a radio telescope does not have an eyepiece), electronic recording of data, and interferometry (to overcome the intrinsically low spatial resolution of

radio telescopes). Many of these techniques are now being applied to telescopes operating at a wide range of wavelengths.

As we study the astrophysics of the Galaxy, the most important characteristic of radio waves is that they readily penetrate dust which is opaque to optical light. This allows us to detect regions of the Galaxy never before studied, and locate the Sun accurately in relation to the overall form of the Milky Way. The measured distribution of radio-emitting gas allows us to trace the structure of the Galaxy. This demonstrates the **spiral structure** of the Milky Way, as illustrated in Figure 2.1. In turn, we can then place the Galaxy in the classification scheme of galaxies in general.

The emission from hydrogen at 21 cm

One of the most important sources of Galactic radio emission comes from the most abundant element in the Universe – hydrogen. See Section 25-3 of *Universe* for another description of the mechanism for this radiation. As with the overall energy of an electron in a hydrogen atom (see Section 4 and Figure 4-9), the **spin** of the electron is **quantised**. The values taken by a quantised physical parameter (energy, momentum, etc.) are restricted; no in-between values are allowed.

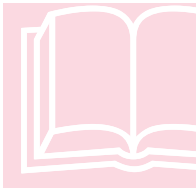
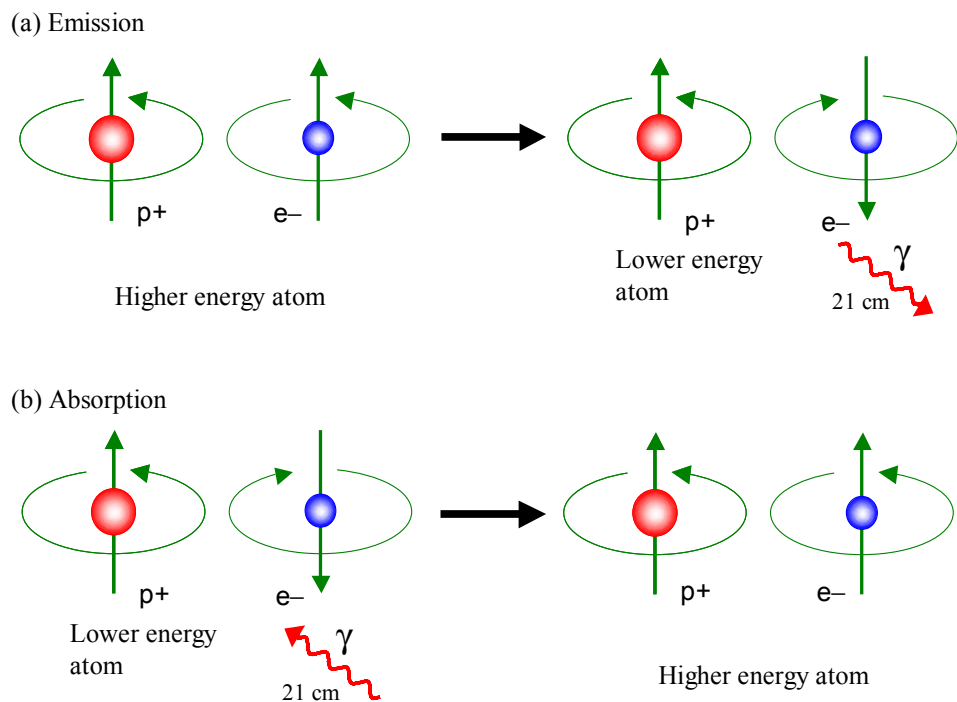


Figure 6.1. Spin-flip transition within a hydrogen atom interacting with a photon (γ) at the radio wavelength of 21 cm. (a) Photon emission as the proton (p^+) and electron (e^-) spins become opposed. (b) Proton and electron spins become aligned following the absorption of a photon.



In the case of spin within a hydrogen atom, it is the relative direction in which the proton and the electron are spinning which is quantised. Essentially, they can either be **aligned** (spinning in the same direction) or **opposed** (spinning in opposite directions). As the aligned state has slightly more energy than the opposed state, the transition between the two releases a photon with an energy equal to the difference – see Figure 6.1. It happens that the energy of this **spin-flip**

transition within the $n = 1$ ground level corresponds to a photon of frequency **1420.406 MHz** or a radio wavelength of **21.1 cm**.

The nature of this spin-flip transition, with a very low transition probability, leads to a line with a very narrow intrinsic width (see Section 2 for an explanation of line emission and spectroscopy). The quantum mechanics which governs changes at the atomic scale also means that the hydrogen atom can only interact in this way with radiation with a wavelength of 21 cm. Consequently, any modifications to the simple, narrow shape of the hydrogen line must be due to the **physical conditions** within the gas, many of which are interesting to us from an astronomical standpoint. The rest of this subsection explains specific application of radio observations at 21 cm. The spectrum of neutral hydrogen (which includes the 21 cm line) is called H I (generally pronounced h-one). Regions in the Galaxy which are dominated by neutral H are called **H I regions**.

Radio “Temperatures”

Radio astronomers define a number of types of temperatures in order to characterise the energy of different aspects of radio-emitting objects. These temperatures can be related to different physical processes that have an impact on the observed lines. This convention derives from the long-standing practice of radio engineers expressing the strength of signals from their receivers as **antenna temperatures**. In all cases, these temperatures represent a measure of energy, as multiplying by Boltzmann’s constant k yields an energy. These definitions have some similarity to the idea of effective temperatures as applied to stars. Several radio astronomical temperatures are relevant to this section:

- **Kinetic** temperature (T) – a measure of the thermal energy within an object (e.g. gas cloud) due to the random motion of its constituent atomic particles. This is identical to the every-day definition of temperature.
- **Excitation** temperature (T_{ex}) – a measure of the energy contained within the atoms prior to its being released as line emission. For example, for the 21 cm transition, this indicates the number of atoms in the higher-energy (aligned) state.
- **Line** temperature (T_L) – effectively a measure of the brightness of each part of a line at a given frequency. This varies with frequency, and we use $T_L(\nu)$ to make this obvious below.

Kinetic temperature and turbulence

One of the physical conditions within any cloud of hydrogen gas that changes the shape of the line is the velocity of motions of gas within that cloud. Although the hydrogen line is intrinsically extremely narrow around the rest frequency of 1420.406 MHz, motions of the atoms within the cloud mean that photons from any given atom can be Doppler shifted to other frequencies. The net result of this happening over all the atoms is that the observed line is broadened.

The MACHO Project

Searches for MACHOs in the Galaxy

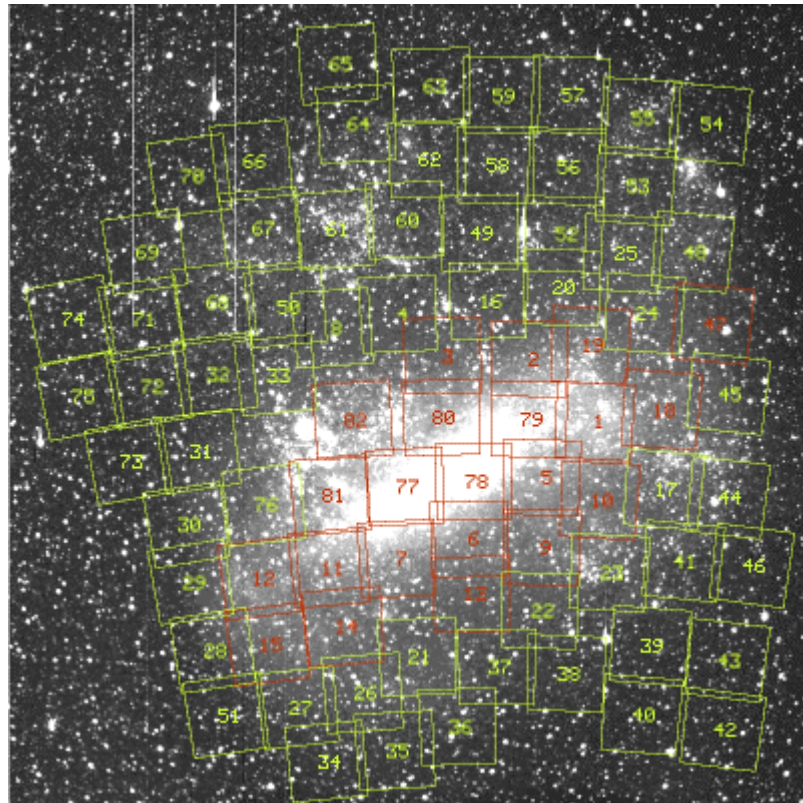
In the last decade a number of surveys have been carried out, seeking microlensing of objects in the LMC or galactic bulge by foreground halo MACHOs. The Macho Project (homepage <http://www.macho.anu.edu.au/>) is a collaboration between Mount Stromlo Observatory (MSO) and the Lawrence Livermore National Laboratory (LLNL) to monitor over 10 million stars in the Large Magellanic Cloud over a period of 8 years of operation. It used large format CCD cameras attached to a dedicated 50-inch telescope (sadly destroyed in the recent bush fires that swept through MSO near Canberra in January 2003) to obtain images in two colours for photometric monitoring. Automatic processing of the thousands of CCD images has since resulted in the detection of 150 lensing events. Of these, the majority of the lenses are in lines of sight to the Galactic bulge, two are towards the Small Magellanic Cloud (SMC) and about a dozen are towards the Large Magellanic Cloud (LMC). The distribution of CCD LMC fields is shown in Figure 7.6 which illustrates the high density of stars in the central regions of the LMC. Given the low probability of a lensing event in the galactic halo, it is a great advantage to the survey to have a large number of background stars to act as potential sources.

Figure 7.6

Fields in the LMC used in the CCD photometric monitoring programme.

Credit:

<http://www.macho.mcmaster.ca/Systems/Coordinates/LMC-Fields.gif>



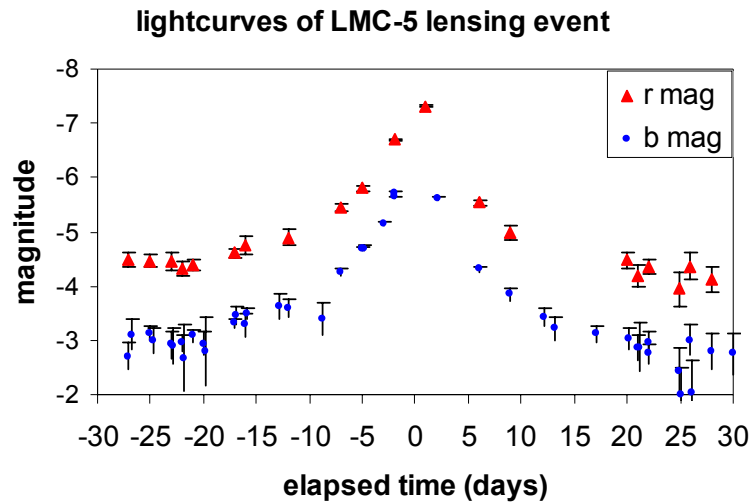
A light curve of a microlensing event LMC-5 is illustrated in Figure 7.7. The light in each of the two colours (b and r) increases by about 3 magnitudes and is symmetrical about the peak to within the observational errors of typically ± 0.2 mag. The overall event lasts about 25 days.

Figure 7.7

Light Curve in b and r of LMC-5 lensing event in February 1993. The b magnitude has been displaced downwards by 1 magnitude for clarity. This plot is based upon public domain data obtained by the MACHO Project

Credit:

<http://www.macho.anu.edu.au/Data/fts.htm>
1

**Direct detection of a microlens**

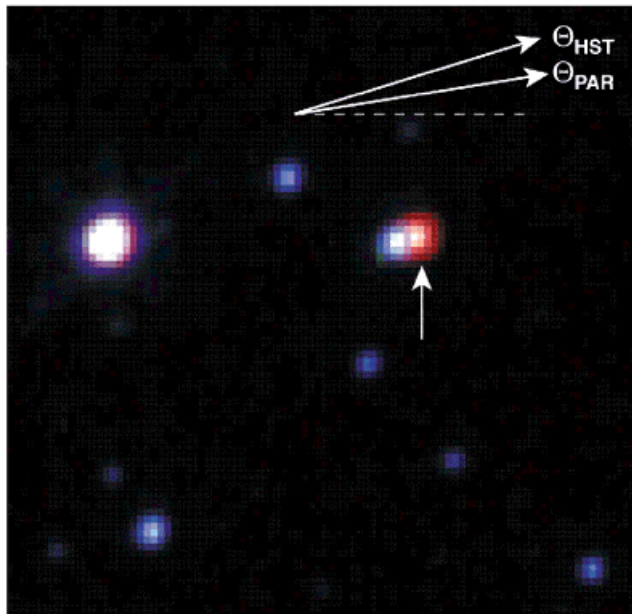
The MACHO Project Team has carried out follow-up observations of the MACHO candidate LMC-5. The observations included HST images in V, R and I (Figure 7.8) and a near infrared spectrum (Figure 7.9) obtained with the ESO Very Large Telescope. These resulted in the first direct detection of a microlens in the Milky Way (Alcock et al 2001, Dec 6, 414, Issue of *Nature*).

Figure 7.8

Three (V, R and I) colour Hubble Space Telescope-image of LMC-5.

Credit:

http://www.llnl.gov/llnl/06news/NewsMedia/macho_images/macho2.jpg



“The microlensing source star is the blue star near the centre of the Figure 7.8 which is partially blended with a much redder object (indicated by arrow) displaced by $0.134''$. The direction of motion of the lens on the sky and the microlensing parallax fit are both shown.” (From original figure caption.)

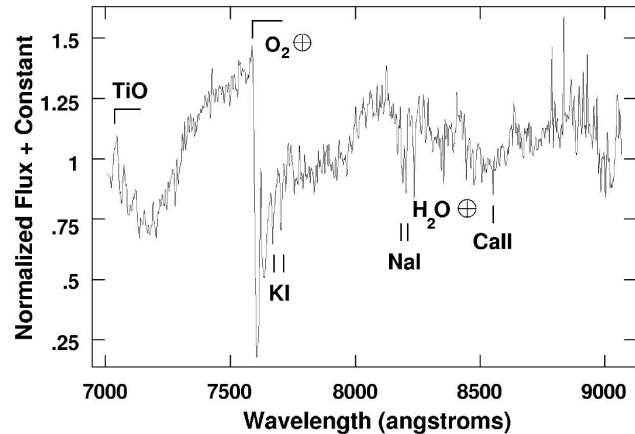
The team assumed that the red object in the image is the lens itself. The ground-based observations were unable to resolve the lens and the background source and consequently the spectrum (Figure 7.9) is a composite of the two objects.

Figure 7.9

Composite FORS2 spectrum of the LMC-5 source lens system.

Credit:

http://www.llnl.gov/llnl/06news/NewsMedia/macho_images/macho3.jpg



“The potassium, sodium and titanium oxide features from the lens are marked. The calcium lines are a blend from both the lens and the LMC source star (spectral type F). The presence of KI, NaI, the absence of CsI +RbI and the TiO band at 7100 Å lead us to conclude that the lens is of spectral type M4-5V.” (From original figure caption.)

In addition, the mass, distance and velocity of the lens reveal that the LMC-5 lensing event was caused by a faint red dwarf at a distance of only 200 pc with U, V and W components of velocity of 27, -43 and -4 kms⁻¹. This indicates that the lens for LMC-5 is a nearby member of the disc population, not the halo. The detection of one such disc lens in their sample of 13 MACHO events in the LMC sample is however consistent with expectations.

Models of halo mass distribution

From the current limited sample of microlensing events it is rather difficult to draw definitive conclusions. Of the dozen or so lensing objects detected in the sightline to the LMC, LMC-5 is probably a Milky Way disc object, and a couple more are probably located in the LMC itself or in a dark halo around our satellite galaxy rather than the dark halo of the Milky Way. Another microlensing event shows the unmistakable signature of a binary lens. That leaves a very small sample with which to answer questions about the overall mass contained in MACHOs in our halo.

Of primary interest is the **MACHO mass function**, that is the number of MACHOs of a particular mass. The absence of large numbers of microlensing events in current surveys that are sensitive down lensing masses of 10⁻⁷M_⊙ precludes significant amounts of mass being distributed as numerous very low mass objects. The predominant view based on the work by Alcock *et al*, is that the majority of events have been due to lensing objects with a mass near 0.5M_⊙ and may account for about 25% of the dark matter in the halo. The low star counts for faint halo objects make it very unlikely that normal stars could account for this. If instead the MACHO candidates were **white dwarfs**, their magnitudes would lie below the limiting magnitude of surveys of star counts to date. However it places severe

Journey to the Centre of the Galaxy

The outermost dark-halo regions of the Galaxy extend to perhaps 200 kiloparsecs from the Centre. At the other end of the range of sizes of Galactic components, the $3 \times 10^6 M_{\odot}$ Black Hole at the core of the Milky Way has a characteristic radius of only ~ 200 nanoparsecs or $10 R_{\odot}$. In this final section of the Module AA2051 we make an imaginary journey from the outer limits to the Galactic Centre, and on the way we particularly investigate our Galaxy's bulge, bar and nuclear regions.

The shape of the Galaxy

From the most extensive component of the Galaxy, the dark halo, we turn now to the innermost regions: the bulge and the Galactic Centre. In this final Section of the module AA2051, we will make the journey from the outermost limits at a radial distance of some 200 kiloparsecs, back through the disc and spiral arms, into the very centre of the nucleus, to the central Black Hole. This has a mass of a few million M_{\odot} within a characteristic radius of only 200 nanoparsecs, or $\sim 10 R_{\odot}$. It will be instructive to make the form of this journey a series of steps on a logarithmic scale. At each step we zoom in by a factor of 10 in linear scale from the previous step.


Step 1. $R \sim 200$ kpc


The **dark halo** fills this region. Within it is the smaller stellar halo of old stars and metal-poor globular clusters. We studied the halo and dark matter in Section 7, and the globular clusters in Section 4.


Step 2. $R \sim 20$ kpc

We zoom in a factor of ten from the outer limits of the dark halo. Here is the familiar **Galactic disc** with its spiral arms, molecular clouds, young stars and open clusters, and here is our solar neighbourhood. We studied these regions in some depth in Sections 2 to 6. The disc rapidly decreases in luminosity as we look back out beyond a radial distance of $R \sim 15$ kpc (S&G p.76). In the inner disc, there is a **concentration of molecular gas clouds** in a fragmented ring at $R \sim 3 - 7$ kpc, with lower concentrations of H_2 inside this (except in the very centre – see later). See S&G Figure 2.20 for a graph of the distribution of H_2 vs. R .


ICON KEY

 Valuable information

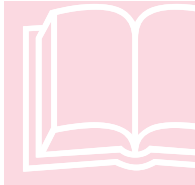
 Test yourself

 Worked example

 Textbook

 Important Equation

The metallicity $[Fe/H]$ of OB stars and H II regions increases with decreasing R in the inner disc. An extrapolation of this relationship yields $[Fe/H] \sim +0.6$ for the Galactic Centre. This is almost certainly due to higher star formation rates and more rapid turnover of material in the stellar evolution cycle (Figure 1.4, Section 1) compared with the solar neighbourhood. A higher dust-to-gas ratio would also be expected towards the Galactic Centre, and this is borne out by the observed higher rates of extinction A_V/kpc towards $l = 0^\circ$.



The next step in our journey will be to zoom in to the region within $R \sim 2$ kpc, including the **Galactic bulge** and the **linear bar**. In conjunction with this and the remaining parts of this Section of Notes, you should read *Se&G* Sections 2.2.4, 2.3.3, 4.3, 4.3.1 and 5.4.3. In addition, *Universe* Section 25-6 gives a good introduction to the Galactic Centre: note in particular Figures 25-7, 25-23, 25-24 and 25-25.

The topics covered in this Section are the subject of dynamic current research programmes. In preparing these Notes Section 8, extensive reference has been made to the following sources and their authors are gratefully acknowledged.

- Chapters 4, 9 and 10 of the Level 4 textbook *Galactic Astronomy* by J. Binney & M. Merrifield, Princeton University Press (1998), ISBN 0-691-02565-7.
- R.F.G. Wyse, G. Gilmore & M. Franx, *Galactic Bulges*, *Ann. Rev. Astr. Astrophys.* **35**, 637 (1997).
- K. Freeman & J. Bland-Hawthorn, *The New Galaxy – Signatures of its Formation*, *Ann. Rev. Astr. Astrophys.* **40**, 487 (2002).
- F. Melia & H. Falcke, *The Supermassive Black Hole at the Galactic Center*, *Ann. Rev. Astr. Astrophys.* **39**, 309 (2001).
- F. Melia, *The Black Hole at the Center of Our Galaxy*, Princeton University Press (2003), ISBN 0-691-09505-1.

You may like to note that the last-named book by Fulvio Melia is a non-technical exposition of the subject written in enthusiastic colloquial American style but also contains much valuable up-to-date material (on Active Galactic Nuclei, relativity and gravity, as well as the main subject) which should be of considerable interest to Level 2 students on this course.

The bulge and the bar

Step 3. $R \sim 2$ kpc

Within a few kiloparsecs of the Galactic Centre lie the Galactic bulge and the central linear bar. In general, the properties of galactic bulges and bars are very closely related and for some galaxies it is difficult to distinguish between them. For example, a prolate-spheroidal (rugby-ball-shaped) structure with its major axis in a galactic disc-plane could be described as either a bar or a prolate bulge.

The Galactic Bulge is “the component constituting the amorphous stellar light in the central regions of the Milky Way.” (Wyse *et al.*, *op. cit.*)

The bulge contributes about 20% of the total bolometric luminosity of the Galaxy. This is closely similar to the average for Sb-Sc type galaxies, whereas for Sa types it is closer to 50%, and is even higher for S0 (lenticular) galaxies.

Figure 8.1 Image of the Galaxy in near-infrared light, taken by the DIRBE instrument on the COBE satellite. Note the asymmetric “boxy” shaped bulge. Image credit: DIRBE/COBE/NASA.



Figure 8.1 shows a **near-infrared image** of the central part of the Galaxy including the bulge. These wavelengths ($\sim 2 - 4 \mu\text{m}$) are optimum for probing the bulge and nucleus because at shorter wavelengths the interstellar dust blocks the starlight whilst at longer wavelengths (e.g. the IRAS far-IR) the emission is dominated by re-radiation from the dust itself. Thus in the near IR the stellar emission can best be seen, although it should be emphasised there is still significant dust extinction which must be allowed for (*cf.* Section 5 of these Notes).

The image shows a flattened bulge of the so-called **“boxy” shape**. In fact it appears to be an ellipsoid with three unequal-length axes – a **triaxial ellipsoid**. About 25% of galactic bulges are of this boxy or peanut-shell shape, with the other 75% having a general elliptical shape. The difference is thought to be due to the presence and orientation of central bars. When a galaxy has a bar and it is viewed approximately edge-on (as opposed to end-on), the bulge shape will appear boxy. If on the other hand a galaxy has no bar or if it has a bar viewed roughly end-on, then the bulge should appear elliptical. Only half of all disc galaxies are barred and the Milky Way is one of them. Furthermore, not all disc galaxies have bulges.

It is important to understand that the bulge cannot be in any sense an extension of the halo or of the disc, because of its distinctive $[\text{Fe}/\text{H}]$ range of values, its higher metallicity than the halo and its younger age than the halo. On the other hand, its angular-momentum distribution is closer to that of the halo than to that of the thin disc or thick disc (see Figure 8.2).

The bulge is denser and more metal-rich than the surrounding disc, and its stars are at least several billion years old. Typical values are $[\text{Fe}/\text{H}] = -0.3$ and ages of